The influence of heating rate on the kinetics of mineral reactions: An experimental study and computer models

Andreas Lüttge,[1,]* Udo Neumann,[2] and Antonio C. Lasaga[1]

[1]Department of Geology and Geophysics, Yale University, P.O. Box 208109, New Haven, Connecticut 06520-8109, U.S.A.
[2]Institut für Mineralogie, Petrologie und Geochemie, Universität Tübingen, D-72074 Tübingen, Wilhelmstrasse 56, Germany

Abstract

Startling results were obtained in kinetic experiments that varied the initial heating history of the mineral reaction: 1 dolomite + 2 quartz → 1 diopside + 2CO_2. The experiments were carried out at 5 ± 0.05 kbar, X_{CO_2} = 0.9, and 680 ± 3 °C, which is 65 °C higher than that of equilibrium. The heating history was varied from the conventional procedure [about 1 h reported by Lüttge and Metz (1991)] by various techniques. The experimental temperature in externally heated cold-seal pressure vessels is attained within 10 min by preheating with a furnace running at 1000 °C, and quickly switching to a furnace set at the temperature of the experiment when T reaches 670 °C. Percent conversion, measured by CO_2 production as a function of time for the period 5 to 288 hours, is linear and fit by the equation, $\alpha = kt$, with $k = 5.64 \times 10^{-2}$ [%conversion/h]. Compared with results produced by the conventional heating procedure, our conversion rate is slower and results show an order of magnitude less scatter. The variation in the magnitudes of the rates measured after the fixed experimental conditions were reached for different heating procedures as well as the large differences in the degree of the scatter of the experimental rate data for different heating procedures are contrary to earlier claims made by most experimentalists and required a rethinking of our kinetic interpretation of the data.

A kinetic model developed to simulate the initial period of a mineral reaction experiment provided a reasonable explanation of many of the unusual facets of the experimental results. The model follows the variation of concentration, ΔG of the reaction, surface area, nucleation rates, and volume of the product as a function of time for the different heating histories used in the experimental study. The key problem ignored in earlier work is the significant effect of a complex nucleation history during the heating conditions on the entire subsequent kinetics, even though the latter are carried out for much longer times and under constant *P* and *T* conditions. Results show that faster heating rates cause faster nucleation rates, and the duration of the nucleation period is shorter. Two different scenarios were compared: (1) a reaction product growing independently of the reactant surface (as may occur in hornfelses with fine grain size); and (2) a reaction product growing on the surface of a reactant. The latter case leads to a significantly reduced reaction rate for faster heating rates (as was observed experimentally), because the surface of the reactant is covered by an armoring rim of product crystals early in the experiment.

Application of the results of this study to natural systems suggests how the kinetics of mineral reactions behave quite differently if there are different nucleation conditions, even if the *P-T-X* conditions of the rock are the same.

Introduction

Although used primarily to study equilibrium conditions of mineral reactions, cold-seal systems also have been employed successfully to investigate the kinetics of many reactions (e.g., Matthews 1980, 1985; Matthews and Goldsmith 1984; Tanner et al. 1985; Champness and Brearley 1986; Heinrich et al. 1986; Schramke et al. 1987; Dachs and Metz 1988; Heinrich et al. 1989; Lüttge and Metz 1991, 1993; for detailed reviews see Rubie and Thompson 1985; and Kerrick et al. 1991). In such studies it is typically assumed that the first few minutes of an experiment would have an insignificant influence on the reaction rate, especially for a duration of days, weeks, or even months. The reason for this assumption is the slow kinetics of most silicate mineral reactions. However, Lüttge et al. (1994) recently reported that the influence of the duration of the heating procedure itself, lasting 30–90 min, may not be negligible. During their experimental study of the initial stage of the decarbonation reaction, 1 dolomite + 2 quartz = 1 diopside + 2 CO_2 (no. 8 in Fig.

* E-mail: andreas@labamba.geology.yale.edu

TABLE 1. Experimental data of conversion vs. time experiments

Sample no.	Duration (h)	Conversion (α)	Initial X_{CO_2}	CO_2 prod. (mg)	Final X_{CO_2}	Solid (mg)
8H/1-00.1	0*	−0.1	0.90	−0.01	0.90	40.11
8H/1-00.2	0*	−0.5	0.90	−0.05	0.90	39.82
8H/1-01.1	5	1.0	0.90	0.11	0.90	39.80
8H/1-02.1	5	1.5	0.90	0.17	0.90	39.95
8H/1-02.2	5	1.6	0.90	0.18	0.90	39.91
8H/1-03.1	29	2.5	0.90	0.29	0.90	39.91
8H/1-04.1	50	3.5	0.90	0.40	0.90	40.02
8H/1-05.1	50	3.3	0.90	0.38	0.90	39.93
8H/1-06.1	70	3.4	0.90	0.39	0.90	40.03
8H/1-07.1	90	4.2	0.90	0.48	0.90	39.89
8H/1-08.1	150	6.6	0.90	0.76	0.91	39.72
8H/1-09.1	288	17.3	0.90	1.98	0.92	39.54
8H/1-23.1	50	15	0.90	1.73	0.91	39.87
8H/1-20.1	150	20.7	0.90	2.36	0.92	39.42
8H/1-20.2	150	22.4	0.90	2.59	0.92	39.97
8H/1-25.1	76†	−0.5	0.90	−0.06	0.90	39.97
8H/1-25.2	76†	3.5	0.90	0.40	0.90	40.37

* "Zero-time" experiment: means only heating and immediately quench, no significant duration at experiment temperature.
† More than 70 h at 605 °C (5 kbar), i.e., 10 °C below the equilibrium temperature of reaction 8 in Figure 1.

1), Lüttge et al. (1994) found that the relatively slow heating rate during the heating procedure seems to be the main reason for scatter in the data. Until now, little work has focused on heating conditions, and especially on their possible influence upon reaction kinetics, although measures such as non-isobaric heating are employed in some cases to avoid fragmentation of solid reactants (e.g., Tanner et al. 1985; Schramke et al. 1987).

The study of the effect of heating conditions on the kinetics of metamorphic reactions is the main focus of this paper. A modified isobaric rapid heating procedure was used to study the influence of heating rate in the heating procedure on reaction rate measurements. The results are compared with: (1) previous data produced by the slower conventional heating method (Lüttge and Metz 1991); and (2) results produced by the rapid heating procedure but with an intentional overshooting of the temperature at the beginning of the experiment.

EXPERIMENTAL PROCEDURE

Optically clear natural dolomite from Algeria (cf. Lüttge and Metz 1991) having an FeO content of 0.7 wt% and synthetic quartz (TOYO company) were used for all experiments. A grain size of 80–100 μm for both reactants was produced by grinding and ultrasonic sieving.

The starting materials and all reaction mixtures have been studied by X-ray powder diffraction (XRD), scanning electron microscopy (SEM), and polarizing microscopy. Comparable SEM-photos of cleavage pieces of dolomite and fragments of quartz from the starting mixtures are given by Lüttge and Metz (1991, 1993).

All experiments were carried out with a solid/fluid ratio of 4:1, using 40 mg of the solid mixture of dolomite and quartz with 10 mg of the fluid phase. The stoichiometry of the reaction requires a mixture of 60.5 wt% dolomite

(24.22 mg) and 39.5 wt% quartz (15.78 mg). Generally, the X_{CO_2} of the fluid phase shifts to higher values during the reaction, because CO_2 is produced by the reaction. In this case, the shift of the fluid composition can be neglected, because it is equal to or smaller than 2 mol% CO_2. Values of X_{CO_2} were determined by gravimetric methods (e.g., Käse and Metz 1980), and the initial and final X_{CO_2} are given in Table 1. Doubly distilled water was used, and the carbon dioxide was produced by the decomposition of $Ag_2C_2O_4$ at the beginning of the experiments. At 140 °C the $Ag_2C_2O_4$ decomposes spontaneously and completely (e.g., Weast 1992), but in our case a significant amount of the silver oxalate is decomposed during the check of proper capsule-sealing in an oven at 110 °C.

The fractional extent of reaction progress, α, was determined gravimetrically: capsules were weighed (no. 1), punctured and weighed again (no. 2), dried at 110 °C in an oven, and then weighed again (no. 3). The difference of the results of no. 1–no. 3 minus the amount of fluid ($H_2O + CO_2$) at the beginning, is assumed to be the amount of CO_2 produced by the reaction. There may be a small amount of H_2O adsorbed on the silver oxalate, but it is in the range of the error of the gravimetric measurement, and therefore, insignificant. From the stoichiometry of reaction (R8), the CO_2 production yields α. This procedure determines, in fact, the amount of dolomite that has decomposed.

All experiments were carried out at 5 kbar and a final temperature of 680 °C in a conventional hydrothermal apparatus using gold tubes (20 mm long, 3 mm diameter) and cold seal pressure vessels (René Allvac 41). The total error in pressure was ±50 bars, measured with a wire resistance strain gauge. Pure CO_2 (99.995%) was used as the pressure medium. The temperature was measured with a calibrated Ni-CrNi thermocouple situated inside each autoclave in direct contact with the central part of the gold capsules. The total error in temperature measurement was ±3 °C.

The composition of the CO_2-H_2O fluid phase was 90 mol% CO_2 and 10 mol% H_2O. The equilibrium temperature (T_{eq}) of the reaction at 5 kbar is 615 ± 10 °C for $X_{CO_2} = 0.90$ (Gottschalk 1997). Thus, T_{eq} was overstepped by approximately 65 °C at the temperature of 680 ± 3 °C. The P-T-X_{CO_2} conditions of each experiment are shown by the square in Figure 1. Duration of the experiments ranged from 5 to 288 h. In addition "zero-time" experiments were performed in which samples were heated up to temperature and then immediately quenched. Heating and quenching procedures were always performed isobarically.

In this study, three sets of experiments were performed using different heating procedures (see Fig. 2): (1) rapid heating rate (9 min to reach 680 °C) without overshooting the temperature; (2) rapid heating rate, but overshooting the temperature for 50 min by up to 10 °C; (3) maintaining temperature at 610 °C for 70 h, (i.e., 5 °C below the equilibrium temperature), then heating quickly to 680 °C
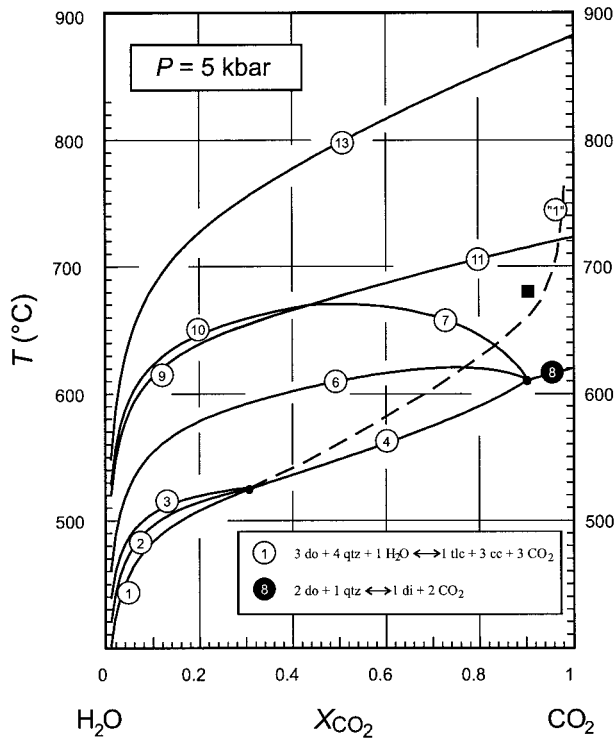
FIGURE 1. Isobaric-T-X_{CO_2} diagram showing reactions occurring in the system CaO-MgO-SiO$_2$-CO$_2$-H$_2$O (Fig. 8.14 in Gottschalk 1990). Curve 1 represents the equilibrium conditions of the reaction: 3 do + 4 qtz + 1 H$_2$O = 1 tlc + 3 cc + 3 CO$_2$, and the dashed line labeled 1 corresponds to its metastable extension. Curve 8 represents the reaction: 1 do + 2 qtz ↔ 1 di + 2 CO$_2$. The black square indicates experimental T-X_{CO_2} conditions. Curve 13 represents the reaction: cc + qtz = wo + CO$_2$ studied by Tanner et al. (1985); for a complete list of reactions see Figure 4 in Gottschalk (1997). Abbreviations: cc = calcite, di = diopside, do = dolomite, qtz = quartz, tlc = talc, wo = wollastonite.

FIGURE 2. Change in temperature with time for experiments using different heating procedures. In all experiments, the equilibrium temperature (T_{eq}) was 615 °C, the final temperature (T_{exp}) was 680 °C, and the pressure was 5 kbar. Dashed line corresponds to conventional heating; solid line to fast heating procedure with no overstep of T_{exp}; dotted line to fast heating with 10 °C overstep of final temperature. In the fast heating procedure, the temperature increase during the heating procedure is nearly linear in the range of 50–400 °C (400 °C is reached within about 3.5 min ± 10 s), T_{eq} is reached within 7 min, and T_{exp} (±3 °C) within 9 min ± 1 min. The dashed line shows that the conventional one-furnace heating procedure requires 23 min to reach T_{eq} and 70 (±10) min to reach T_{exp}, respectively. The large uncertainty of ±10 min is caused by the slow approach to T_{exp} and slight variations in the position of the autoclave within the furnace from experiment to experiment.

without any overshoot, and maintaining this temperature for 36 h. Results were compared with experiments performed with the conventional slow heating procedure (Lüttge and Metz 1991) in which heating to 680 °C was done in at least 50 min (Fig. 2).

The rapid heating procedure was achieved by using two furnaces that were physically interchanged as the experiment approached the temperature of the experiment. The first furnace was heated to 1000 °C. The second furnace was set at the exact temperature (680 °C). The temperature for the interchange of furnaces must be determined by trial and error for each experimental temperature. By carefully adjusting the time of interchange, the experimental temperature (±3 °C) can be reached without any "overshoot" (see Fig. 2; note that the term "overstep" is used for the interval between the equilibrium and the experimental temperature, whereas the term "overshoot" is used for an increase of temperature above the experimental temperature). In this study, the furnaces were interchanged at 670 ± 3 °C. During
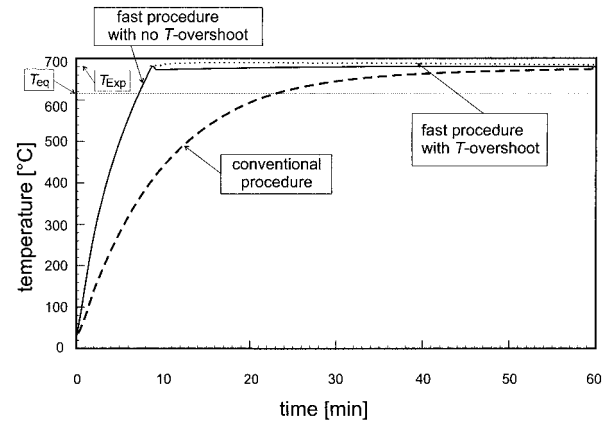
the whole heating time, the pressure is controlled and regulated to maintain isobaric conditions (±10 bar).

RESULTS

SEM studies of all reaction mixtures show needlelike crystals of newly formed diopside growing exclusively on the surface of dolomite (Fig. 3A). Quartz grains are always free of any precipitation products (Fig. 3B). All reactants show dissolution features like rounded edges and corners, etch pits, and dissolution hillocks (exclusively on quartz). These results are in complete agreement with observations of Lüttge and Metz (1991; Figs. 3A–D) who also reported small amounts of metastable talc crystals covering the surface of dolomite (see talc tiles in Fig. 4C of Lüttge and Metz 1991). The formation of metastable talc and calcite was also observed in all experiments of the present study (Figs. 3C and 3D). These metastable minerals are probably formed by the reaction, 3dolomite + 4quartz + 1H$_2$O → 1talc + 3calcite + 3CO$_2$, which is also overstepped (no. 1 in Fig. 1). However, the amount of metastable products was so small in our experiments that they were not detectable with XRD. Large amounts of metastable talc and calcite, along with minor diopside crystals, were observed in experiments 8H/1-25.1 and 8H/1-25.2 (Fig. 3D), which were held below the equilibrium temperature for 70 h before heating up to 680
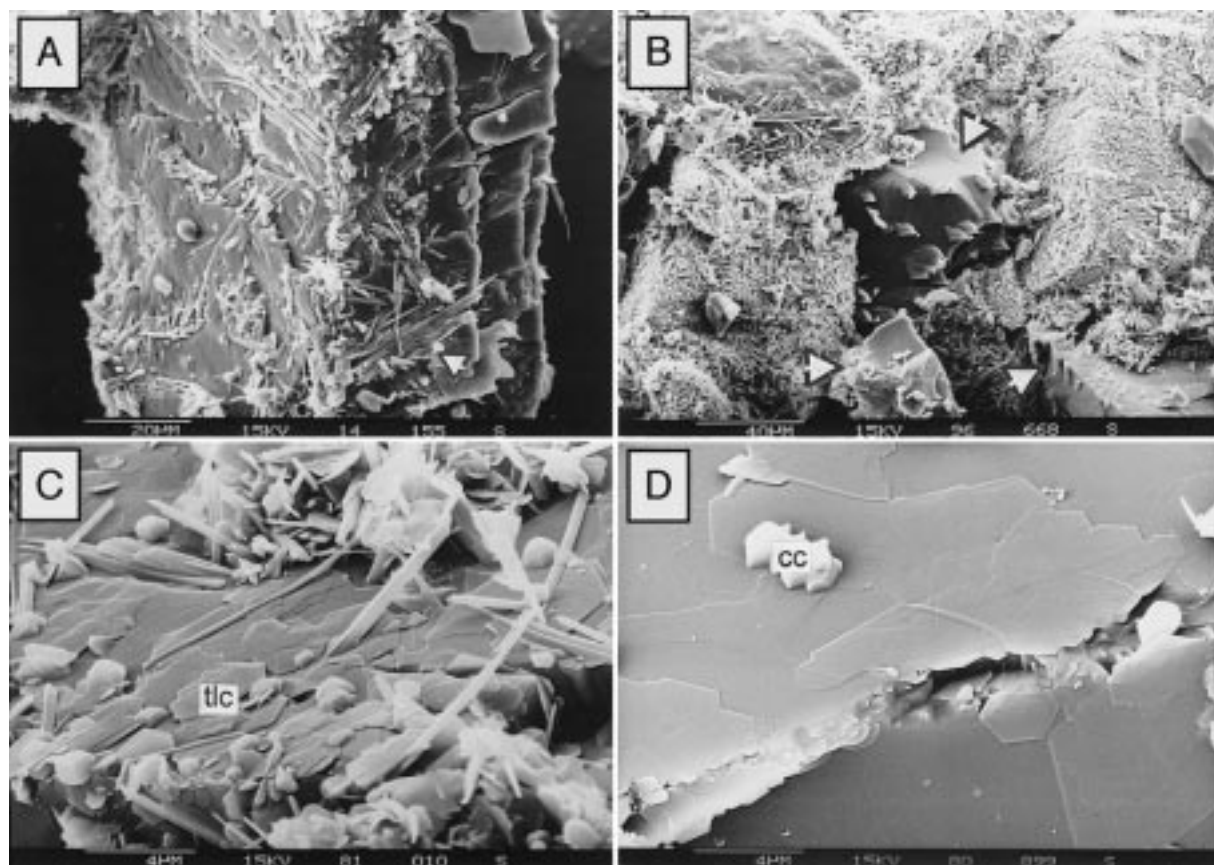
FIGURE 3. SEM photomicrophotographs. (**A**) Diopside crystals with a needle-like shape growing exclusively on the surface of the dolomite (e.g., lower right). (**B**) Surfaces of quartz grains free of diopside (arrows). The quartz surfaces commonly show crystallographically oriented hillocks produced by the dissolution process; (**C**) Talc plates and calcite mounds intergrown with diopside crystals; (**D**) Plates of talc covering the dolomite surfaces like tiles.

°C and maintaining it for 76 h. The degree of fragmentation of the reactants dolomite and quartz was evaluated by SEM, and found to be small in all cases (< 5%, cf. Lüttge and Metz 1991), even in the ''zero-time'' experiments.

All experimental data and results are given in Table 1. The conversion vs. time data for the experiments performed with the rapid heating procedure, but without a temperature overshoot, are compared with data obtained using the slow heating technique by Lüttge and Metz (1991) in Figure 4. Faster heating produces a significantly slower reaction rate and a decrease in the scatter of data points by an order of magnitude. Experiments performed with the rapid heating method also show significantly improved reproducibility (±1% scatter in the reaction rate). The conversion rate corresponds to the lowest values of Lüttge and Metz (1991).

The regression line in Figure 4 (for the data of this study only) was determined by least-squares methods. The rate law can be assumed to be linear (zeroth order):

$$\alpha = kt \qquad (1)$$

during the first few hundred hours duration of the exper-

iment as long as T and X are constant, and the surface area of reactants does not change significantly. Another assumption is that the rim of diopside crystals is not armoring the dolomite (see discussion in Lüttge and Metz 1991). The rate constant, k, which corresponds to %conversion/h, is 5.64×10^{-2}.

Figure 4 also presents additional data produced by a temperature overshoot of 10 °C, i.e., a temperature of 690 °C during the first 50 min of the experiment. The temperature overshoot of 10 °C is only about 1% of the total temperature of the experiment (953 K) and an increase of about 15% of the regular temperature overstep (65 °C). The overshoot duration, 50 min, represents only 1.7% and 0.6% of the total duration of the experiments (50 and 150 h, respectively). These results show an increase of reaction rate by 300% compared with rapid heating with no overshoot.

DISCUSSION OF EXPERIMENTAL RESULTS

It is typically assumed that variations in the duration of heating in experiments will not significantly affect the rates of metamorphic reactions, because initial heating lasts no more than several tens of minutes, while exper-

imental durations are typically tens to hundreds or thousands of hours, which is several orders of magnitude longer than the heating period. However, the experimental data summarized in Figure 4 strongly suggest that initial heating rate has two significant effects on experimentally determined reaction rates: (1) the decrease of reaction rate with increasing heating rate; and (2) the decrease of scatter in the conversion vs. time data by an order of magnitude for the fast heating rate. The variation in reaction rate as a function of heating rate during the initial behavior is important for determining k and the apparent activation energy in the case of zeroth-order kinetics (e.g., Lasaga 1981; Heinrich et al. 1989). The decrease of reaction rate can be observed even after about 290 h (see Fig. 4, and Table 1, 8/H/1-09.1). Furthermore, the results of the experiments both without overshooting the temperature of the experiment (8/H/1-01.1–8/H/1-09.1) and with temperature overshoot (8/H/1-20.1, 8/H/1-20.2, and 8/H/1-23.1) show that the influence of starting conditions is very important. Obviously, this effect cannot be eliminated later, even if temperature fluctuations occurring after reaching the desired experimental conditions are avoided.

One possible factor in the observed kinetic behavior, which could affect the reaction rate as well as the scatter in the conversion vs. time data is grain fragmentation of reactants, especially if there is a variation in the degree of fragmentation from one experiment to another. This is also a reason why the direct applicability of powder experiments to natural rocks has been criticized (e.g., Rubie and Thompson 1985).

A scatter of experimental data in the range of ±5–10% was reported by Tanner et al. (1985) for the reaction, calcite + quartz ↔ wollastonite + CO_2 (no. 13 in Fig. 1). These authors were very concerned about fragmentation of their starting material and thus developed a non-isobaric heating procedure, which includes a time span at 170 °C and 1 atm to decompose the $Ag_2C_2O_4$. This procedure guarantees true hydrostatic pressure conditions ($P_{total} = P_{fluid}$) even at the very beginning of the experiment and, therefore, prevents fragmentation. However, a review of the results provided by their non-isobaric method shows that the scatter of data is still in the range of about 5–10% (see Fig. 6 in Tanner et al. 1985).

Another source of scatter may arise from the additional surface area of small particles of reactant material produced during grinding, and situated on the surfaces of the larger reactant grains. Different methods have been proposed to prevent this: cleaning the surfaces of reactants after grinding by sonic cleaning with alcohol or acetone, as well as acid-etching the surfaces of the reactants (e.g., Schramke et al. 1987). However, the latter method has the drawback that etching may influence the reaction kinetics (Neumann and Lüttge 1995).

In the present study and that of Lüttge and Metz (1991), the degree of fragmentation and/or fine particles on the surfaces of the reactants cannot be the reasons for the scatter of experimental data. The latter study had in
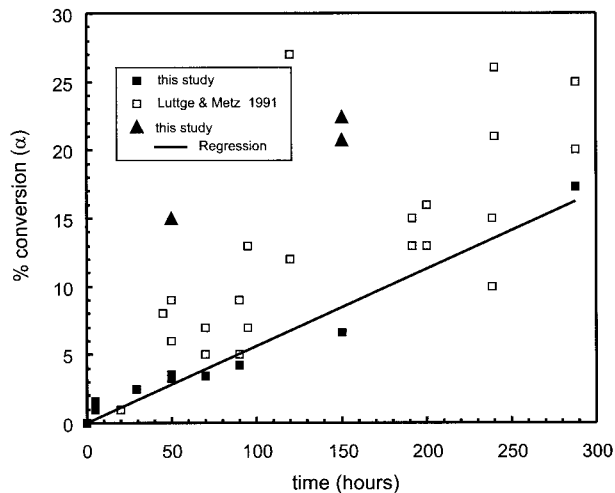

FIGURE 4. Conversion (α) vs. time data for the reaction, 1 dolomite + 2 quartz → 1 diopside + 2 CO_2. Black squares show the data of this study. Open squares show the scattering of data produced with the conventional heating procedure (Lüttge and Metz 1991). Black triangles show the results of experiments with a 50 min temperature overshoot of 10 °C. The straight line was calculated by linear regression, ($R = 0.95$). The analytical error of all conversion data is in the range of the symbol size.

fact a large range of scatter (±5–10%, open squares in Fig. 4), but only a small degree of fragmentation. This was proven by studying the solid starting material as well as powders of "zero-time" experiments with the SEM (compare also to Figs. 4A and 10B, E in Lüttge and Metz 1991). The starting material for all experiments was cleaned ultrasonically such that only an insignificant amount of fine particles was present on the surface of the reactants (compare also to Lüttge and Metz 1991, Fig. 1B). Because we used the same starting materials, sample preparation, pressure increase, and loading procedures as Lüttge and Metz (1991), the degree of fragmentation is unlikely to account for the difference in the scatter of the data between these studies.

However, any number of fragments and/or fine particles sitting on the surfaces of the reactants, as well as dislocations produced during the grinding process, will produce a higher reaction rate compared with a reaction mixture without any fragments, due to the higher surface area of reactants. Non-isobaric heating-up procedures, leaching and/or annealing of surfaces by tempering will decrease this effect. This is in good agreement with the experimental results of Tanner et al. 1985 (Fig. 3) and of Schramke et al. (1987).

An indirect effect of the heating procedure on the kinetics of the mineral reaction involves the decay of the silver oxalate that is used to produce the CO_2 in the sample charge. The decomposition of silver oxalate according to the reaction, $Ag_2C_2O_4 \rightarrow 2Ag + 2CO_2$, occur spontaneously at 140 °C and 1 atm (e.g., Weast 1992). From "zero-time" experiments performed in an internally heated

gas vessel (Lüttge et al. 1994), we know that the spontaneous decay of the oxalate occurs also at least up to 5 kbar—even if it might happen at somewhat higher temperatures. A significant portion of the oxalate is already decomposed during the test for leakage (see the Experimental method section; this is probably the reason for the small amount of fragmentation). Therefore, no significant effect on the reaction kinetics can be expected by the decomposition of the oxalate during the different heating procedures used in this study.

The effect of the talc- and calcite-forming parallel reaction ($R1$ in Fig. 1) on the kinetics of the diopside-forming reaction was not investigated in particular (Figs. 3C and 3D). The metastable formation of talc (calcite) during diopside or tremolite formation is common at least in experimental studies and was described before by Lüttge and Metz (1991) and Lüttge and Neumann (1993). However, talc (calcite) was observed in all experiments, and there are no indications that the amount of talc (calcite) produced differs significantly from one experimental procedure to the other.

A different behavior was observed when we kept experiments slightly below the equilibrium temperature for 70 h (8H/1-25.1 and 8H/1-25.2). In this case talc was formed already, which is a difficult problem to explain because the temperature of 605 °C is even below the metastable extension of reaction (R1). In general, such a two-step heating procedure could help to attain more reproducible starting conditions, because equilibrium should be achieved between the reactants and the solution without any diopside formation. The uncertainty of heating from slightly below the equilibrium temperature (e.g., 605 °C) to the final temperature of the experiment (680 °C) should be much smaller than when it is increased all the way from 25 °C. Due to metastable talc formation, this procedure cannot be used in the present case, but it might be suitable for other reactions that occur without the complication of metastable phase formation.

Consequently, we conclude that the difference in heating rate is the most likely reason for the observed differences in reaction rate as well as for the scatter in the experimental data. This conclusion is supported by additional experiments, in which a controlled, reproducible overshoot using the fast heating procedure illustrates the effect of an overshoot on the reaction kinetics. The maximum temperature overshoot was 10 °C (690 °C) during the first 50 min. This period lies between 0.6 and 1.7% of the total durations of the experiments. The results of these experiments show an increase of at least 300% in the reaction rate compared with the experiments without a temperature overshoot (Figs. 2 and 4). Although there are no experimental measurements that can be used to explain the dramatic increase in reaction rate (by a factor of about 3 to 4.5), we suggest it is caused by a significant increase in the diopside nucleation rate. The large increase in the overall reaction rate is reasonable only if a significant number of additional nuclei are formed and subsequently grow. Otherwise, the growth rate of the di-

opside crystals needs to increase by a factor of at least 3, which seems highly unreasonable. This interpretation agrees with the results of Lüttge and Metz (1991) who argued that the precipitation of diopside is rate limiting from the beginning of the reaction until the surface area of the reactant(s) is reduced to where the dissolution becomes rate determining. This conclusion is supported by the results of our kinetic model presented in the next section. However, the experimental results show that special care is necessary when performing the heating procedure in this type of high-temperature experimental study.
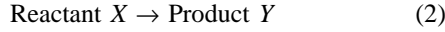
Our experimental observations, including both the effect on the scatter in the rate data and the variation in the magnitude of the rate itself, were unexpected and certainly contrary to what most previous investigators would have predicted. Therefore, a re-thinking of the key kinetic variables and processes was required. Models based solely on kinetics of growth and dissolution are consistent with the earlier ideas but could not explain these new observations. On the other hand, if a coupling of nucleation and growth was essential to the final growth kinetics, effects such as those observed may be explained under some circumstances. To find out if that was possible, a kinetic model was needed that dealt with both nucleation and growth. Because of the non-linearities of the rate laws (especially nucleation), such a model necessitated a numerical approach.

KINETIC MODEL

A kinetic model must account for several important parameters that cannot be measured as a function of time or temperature for conventional cold seal experiments using sealed capsules, such as the concentrations of dissolved species and the surface areas of the reactants and products. These parameters are important because they determine the kinetics of the system. In particular, the Gibb's free energy of reaction, ΔG_r, has been shown to have a dramatic effect on the kinetics (e.g., Nagy and Lasaga 1992; Burch et al. 1994). We already know from our experiments (e.g., Lüttge and Metz 1991) that the overall reaction studied proceeds by a dissolution-precipitation mechanism; however, the effect of nucleation must be included in our model. The systems of relevance to both nature and laboratory involve the nucleation and growth of several minerals as well as the simultaneous breakdown and dissolution of several others. Therefore, a fully realistic model of these reactions would involve many mineral phases interacting with a fluid phase. Although future models will incorporate such a multitude of phases (e.g., as in Lasaga and Rye 1993), the authors believe that the underlying chemistry and physics governing the important results of the laboratory studies reported here can be elucidated quite well by focusing initially on a simpler system involving one phase that is breaking down and another new phase that is nucleating and growing, both in the presence of a fluid phase. Once the salient features of the laboratory data are explained, as this paper will do, the actual results can and should be

compared with more sophisticated models involving many phases. Nonetheless, the interplay of homogeneous vs. heterogeneous nucleation, the role of nucleation overstepping, the effect of surface coverage by new products, and the kinetic control of the thermal history (of the laboratory experiments in our case and of Mother Nature in the implications of the paper) can be initially understood best with the approach that we have taken here.

Our kinetic model, therefore, focuses on the simple reaction:

$$\text{Reactant } X \rightarrow \text{Product } Y \qquad (2)$$

involving only two minerals in a closed system: One reactant X that dissolves and one product Y that both nucleates and grows as the solution becomes supersaturated with respect to its equilibrium concentration, $c_{Y,\text{eq}}$. We want to base the model on well-known kinetics. Therefore, as an example we have chosen silica gel (X) and quartz (Y) as solid phases used in the model (single-mineral kinetic data for diopside and dolomite are not available).

In this model, there are two possible surface reactions that effect the concentration of a dissolved component in the fluid, the dissolution of reactant X and the growth of product Y. Therefore, the change in concentration of a dissolved component (e.g., H_4SiO_4) as a result of both of these heterogeneous processes is given as

$$\frac{dc_i}{dt} = \frac{A_X}{M_f}k_X\left(1 - \frac{c_i}{c_{X,\text{eq}}}\right)^m + \frac{A_Y}{M_f}k_Y\left(1 - \frac{c_i}{c_{Y,\text{eq}}}\right)^n \qquad (3)$$

where dc_i/dt is the change of the concentration (mols/g) of species i in the solution with time; A_X and A_Y are the surface areas of X and Y (cm²), respectively; M_f is the mass of the fluid (g) (see Rimstidt and Barnes 1980). Note that A_X and certainly A_Y are strong functions of time. The variables k_X and k_Y are the rate constants of dissolution far from equilibrium for solid phases X and Y, respectively (mols/cm²s). The variables $c_{X,\text{eq}}$ and $c_{Y,\text{eq}}$ are the equilibrium concentrations of species, i, with respect to mineral X and Y, and are functions of temperature. The reaction order m can be any constant, although linear kinetics ($m = n = 1$) are assumed for simplicity. The term $(1 - c_i/c_{\text{eq}})m$ incorporates the necessary and important dependence of the rate on ΔG_E. [Note that from transition state theory (TST) it follows (e.g., Lasaga 1998): $f(\Delta G_e) = 1 - e^{\Delta G/RT} = 1 - \exp(\ln IAP/K) = 1 - IAP/K$, where IAP is the ion activity product, and K is the equilibrium constant. Assuming that the activity coefficients are equal to 1 (very dilute solution), $f(\Delta G_E) = 1 - \frac{c_i}{c_{eq}}$]. For the case where X is silica gel and Y is quartz, the dependence of the rate constants and the equilibrium concentrations, $c_{X,\text{eq}}$ and $c_{Y,\text{eq}}$, as a function of temperature are taken from Rimstidt and Barnes (1980). [For a thorough review of kinetic behavior of the system silica-water, the reader is referred to Dove and Rimstidt (1994)].

In general, experimental investigations into the mechanisms of heterogeneous mineral reactions have shown

that two different nucleation scenarios are observed: (1) homogeneous nucleation of product crystals that grow independently of the surfaces of the reactant(s); and (2) heterogeneous nucleation of product(s) that grow on the surface of the reactant(s) (e.g., Tanner et al. 1985; Dachs and Metz 1986; Lüttge et al. 1991, 1993; Widmer et al. 1995; Winkler and Lüttge 1997). Fluid composition seems to be an important parameter in controlling the nucleation mechanism: Even if the majority of experimental studies have shown heterogeneous nucleation to be much more common, homogeneous nucleation might be an important consideration in cases of an H_2O-rich fluid. For example, Heinrich et. al. (1986, 1989) showed experimentally that forsterite crystals grow independently of dolomite (reactant) surfaces if the fluid contains only relatively small amounts of CO_2 (10–40 mol%). If the CO_2-content is larger than 40 mol% the forsterite grows on the dolomite surfaces.

Homogeneous nucleation

In this case, it is assumed that the surface area of reactant X, A_X, is not overgrown by any product and, therefore, there is no reduction in the surface area of X. The amount of the reactant that will become dissolved in the fluid is small as long as only the initial period of the reaction is considered. Thus, A_X/M_f is assumed constant during the initial period:

$$\frac{A_x}{M_f} = \text{constant} = (A_X^* M_X)/M_f \qquad (4)$$

where A_X^* is the specific surface area of silica gel (taken from Rimstidt and Barnes 1980), M_X is the mass of X in the beginning of the experiment (here 40 mg, Table 1).

The surface area of mineral Y, A_Y, changes dramatically during the initial period of the experiment, and therefore, must be calculated as a function of time. To do so, we must take into account nucleation and growth of the product crystals. The nucleation rate can be expressed as:

$$I_{Y,n} = p_{Y,n}\exp\left\{-\frac{E_{Y,n}}{RT}\right\}\exp\left\{\frac{-69.3\overline{V}^2\sigma^3}{T\Delta G_r^2}\right\} \qquad (5)$$

where $I_{Y,n}$ is the rate of formation of nuclei (nuclei/s), $p_{Y,n}$ is a preexponential factor (nuclei/s), $E_{Y,n}$ is the apparent activation energy of nucleation of Y (J/mol), and R is the gas constant (for a derivation, see Lasaga 1998). [We use the term "apparent" activation energy, because an overall mineral reaction consists of many elementary reactions, which all have their own specific activation energy (cf. Matthews 1980; Rubie and Thompson 1985)]. The last exponential involves the molar volume, $\overline{V}$ (cm³/mol), the free interfacial energy, σ (ergs/cm²), the temperature, T (kelvin), and the Gibb's free energy of the reactions, ΔG_r (cal/mol). The constant, -69.3, assumes that $\overline{V}$, σ, and T are in the units given (see Lasaga 1997).

Assuming Arrhenius behavior for the rate constants in Equation 3,

TABLE 2. List of input data used for the simulation

Timestep	0.1	s
No. of timesteps	40 000	
Max. time	70	min
Starting T	293.15	K
=	20	°C
T of experiments	953.15	K
=	680	°C
Mass of fluid	1.0×10^{-5}	kg
Mass of mineral X	4.0×10^{-5}	kg
Spec. surface area of X	1.1×10^3	m²/kg
Molar volume of $X2$	24.0	cm³/mol
Spec. volume of Y	22.0	cm³/mol
Initial concentration	1.0×10^{-30}	mole/kg
l_1, l_2, l_3 dimensions of X grains	0.01, 0.01, 0.01	
Heating history	1 (slow), or 2 (fast), or 3 (very fast)	
Activation energy of dissolution of		
X	60 000	J/mol
Preexp. factor	0.036	mols/m²s
Activation energy of nucleation of		
Y	5000	cal/mol
Preexp. factor	2.0×10^{35}	nuclei/cm³s
Activation energy of dissolution of		
Y in l_1 direction	80 000	J/mol
Preexp. factor	7.0	mols/m²s
Activation energy of dissolution of		
Y in l_2 direction	80 000	J/mol
Preexp. factor	10.0	mols/m²s
Activation energy of dissolution of		
Y in l_3 direction	80 000	J/mol
Preexp. factor	5.0	mols/m²s

$$k_X = p_{X,d}\exp\{-E_{X,d}/RT\} \qquad (6a)$$

$$k_Y = p_{Y,g}\exp\{-E_{Y,g}/RT\} \qquad (6b)$$

the vertical rate of growth, r_g (m/s), of the crystal surfaces (see Lasaga 1984) is given by

$$r_g = -\overline{V}10^{-6}p_{Y,g}\exp\{-E_{Y,g}/RT\}\left[1 - \frac{c_i}{c_{Y,eq}}\right] \qquad (7)$$

where, $\overline{V}$ is the molar volume of Y (cm³/mol), $p_{Y,g}$ is a preexponential factor (mols/m²s), and $E_{Y,g}$ is the apparent activation energy of the growth (J/mol). To study the influence of different heating histories or other parameters, it is convenient to compare relative rates of conversion of the product. The extent of conversion can be expressed as the value of the total surface area of Y or the volume of Y as a function of time. Using Equations 5 and 7, the surface area, A_Y, for spherical Y crystals can be calculated from:

$$A_Y = \int_0^t I_{Y,n}(\tau)4\pi\left(\int_\tau^t r_g(t')\,dt'\right)^2 d\tau. \qquad (8)$$

We note that the integral $\int_\tau^t r_g(t')dt'$, in which t' and τ are dummy integration variables of time, gives the size of the particles at a certain time. The evolution of the surface area is calculated by the integral of the nucleation rate for a particular time τ (for the time interval σ to t) times the surface area of the crystals nucleated at that time, $4\pi(\int_\tau^t r_g(t')\,dt')^2$. Similarly, the total volume of Y as a function of time can be calculated from

$$V_Y = \int_0^t I_{Y,n}(\tau)\frac{4}{3}\pi\left(\int_\tau^t r_g(t')\,dt'\right)^3 d\tau \qquad (9)$$

where V_Y is the volume of all Y crystals (cm³) formed at a certain time, t.

Table 2 presents the input data used for the calculations. The model also requires thermal histories, which were calculated by polynomial fits of the three different real heating rates used during the experimental studies. Figure 5 shows the results of the model calculations. In Figures 5A and B, the dashed and the solid lines show the change of silica concentration in the solution as a function of time for the slow and the fast heating procedure, respectively. The double dotted dashed lines give the equilibrium concentration with respect to X (silica gel), and the dotted lines give the equilibrium concentration with respect to Y (quartz) as a function of time. Note that a heating procedure is considered, and therefore, the equilibrium concentration will vary with time. Figure 5C gives the nucleation rate of Y as a function of time, while Figure 5D compares the development of ΔG with time for the fast and the slow heating procedure. In particular, Figures 5E and 5F show that the surface area produced as well as the volume of Y is higher in the case of a fast heating rate. (This is true for a wide range of free interfacial energy, σ; 50–500 ergs/cm²). Therefore, it is quite clear from these results that a model involving homogeneous nucleation does not explain the experimental results.

Heterogeneous nucleation

As a second model, the product Y was allowed to grow on the surface of the reactant X. As a consequence of the increased armoring overgrowth by the product crystals, the (reactive) surface area A_X no longer can be assumed to be constant as in the first model, and will decrease significantly during the experiment. Figure 6 is a sketch that shows the situation considered in this approach. It is assumed that the product crystals are orthorhombic, where l_1, l_2, and l_3 are the sides of a parallelepiped. The volume, V_Y, of each parallelepiped is given by

$$V_Y = l_1 l_2 l_3 \qquad (10)$$

and the total surface area, A_Y, of each crystal (including the area on top of the reactant, X) can be calculated from

$$A_Y = 2l_1 l_3 + 2l_2 l_3 + 2l_1 l_2 \qquad (11)$$

The growth rates in the l_1, l_2, and l_3 directions of each crystal are given by Equations 12a–c:

$$\frac{dl_1}{dt} = k_{l_1}f_{l_1}(\Delta G)\overline{V}_Y \qquad (12a)$$

$$\frac{dl_2}{dt} = k_{l_2}f_{l_2}(\Delta G)\overline{V}_Y \qquad (12b)$$

$$\frac{dl_3}{dt} = k_{l_3}f_{l_3}(\Delta G)\overline{V}_Y \qquad (12c)$$

where k_{l_1}, k_{l_2}, and k_{l_3} are the rate constants in the l_1, l_2,

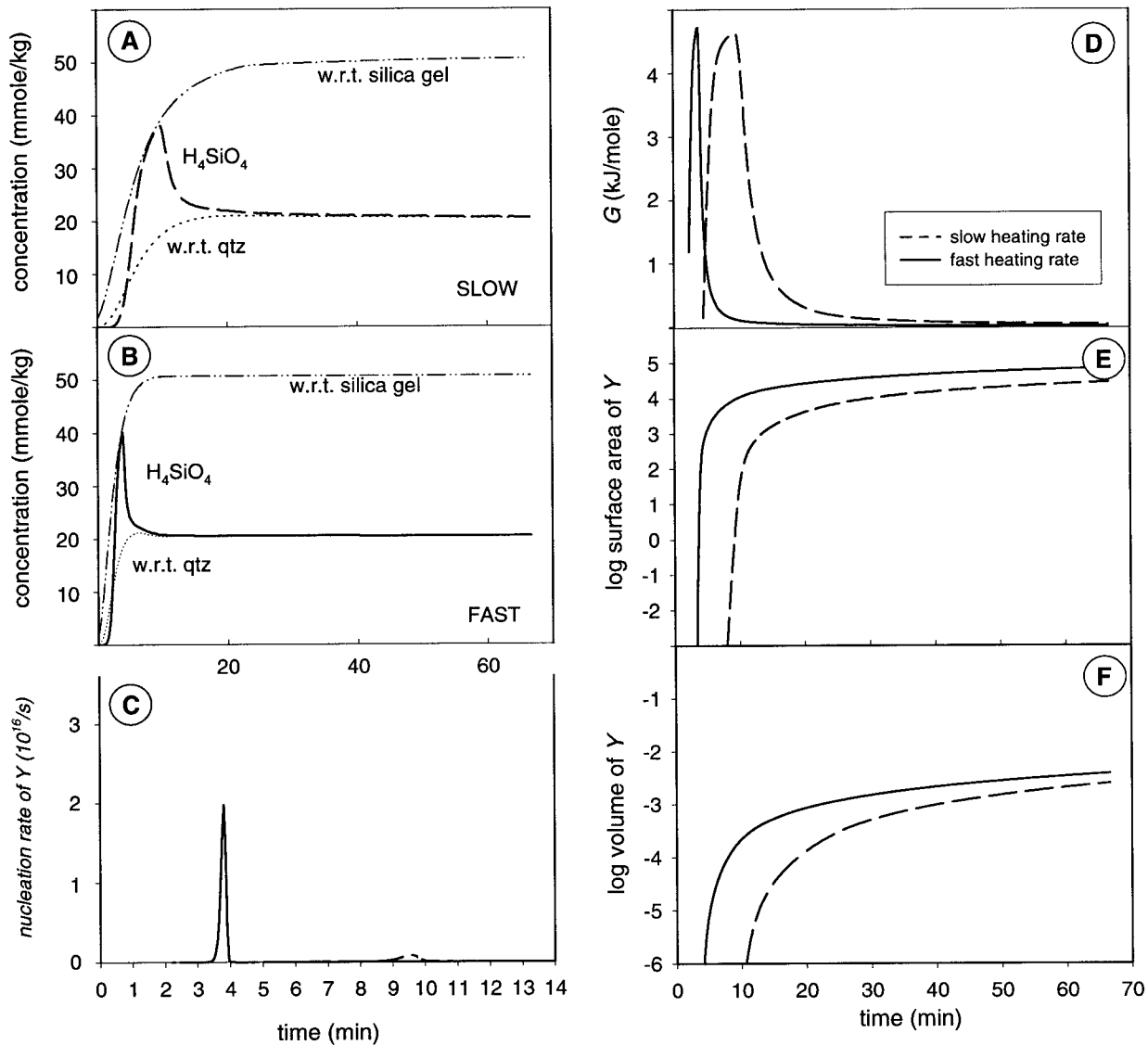## Homogeneous Nucleation

FIGURE 5. Results of the simulation, assuming homogeneous nucleation of *Y,* i.e., the product (quartz) is not growing on the surface of the reactant, *X* (silica gel); results of slow heating procedure (dashed lines), results of fast heating procedure (solid lines). For more detailed discussion see text. (**A**) Equilibrium concentrations of *X* (double dotted dashed line) and *Y* (dotted line) as a function of time (temperature), and the development of the concentration of $H_4SiO_{4,aq}$ caused by the slow heating procedure; (**B**) Equilibrium concentrations of *X* and *Y* as a function of time (temperature), and the development of the concentration of H_4SiO_4 in the solution caused by the fast heating procedure; (**C**) Comparison of the nucleation rates of *Y* as a function of time for the slow and the fast heating procedure; (**D**) ΔG-values as a function of time; (**E**) Production of surface area of *Y* as a function of time; (**F**) Production of volume of *Y* as a function of time. (The surface area is calculated in square centimeters, and the volume is calculated in cubic centimeters.)

and l_3 directions, respectively. [The form of the ΔG functions, $f_{l_1}(\Delta G)$, $f_{l_2}(\Delta G)$, and $f_{l_3}(\Delta G)$, depends on the reaction mechanism(s) (see Lasaga et al. 1994 for a detailed discussion) and might be provided by experiments measuring reaction rates of oriented crystal surfaces (rotating disk experiments, e.g., MacInnis and Brantley 1992), atomic force microscopy and scanning force microscopy (e.g., Bosbach and Rammensee 1994; Dove and Hochella 1993; Gratz et al. 1991; Putnis et al. 1995; Stipp et al. 1994), or optical methods (Lüttge et al. 1996; MacInnis
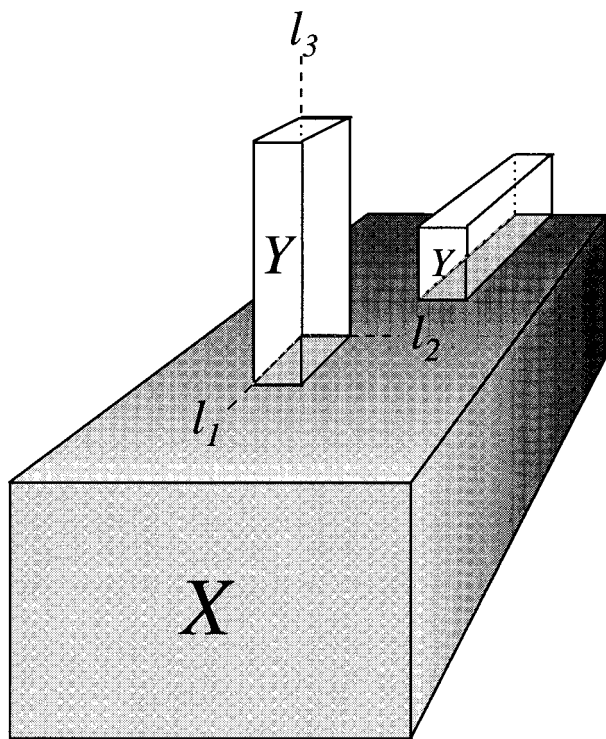
FIGURE 6. Sketch showing crystallographic consideration for the simulation assuming heterogeneous nucleation (product crystals are growing on the surface of a reactant).

et al. 1996)]. Using Equations 12a–c, Equation 9 for the total volume, V_Y, of the product crystals as a function of time becomes:

$$V_Y = \int_0^t I_{Y,n}(\tau)\left[\left(\int_\tau^t \frac{dl_1}{dt}\,dt'\right)\left(\int_\tau^t \frac{dl_2}{dt}\,dt'\right)\left(\int_\tau^t \frac{dl_3}{dt}\,dt'\right)\right]d\tau$$

(13)

and the individual surface areas for l_1l_3, l_2l_3, and l_1l_2 faces of the boxes, $A_{l_1l_3}$, $A_{l_2l_3}$, and $A_{l_1l_2}$ are

$$A_{l_1l_3} = \left(\int_\tau^t \frac{dl_1}{dt}\,dt'\right)\left(\int_\tau^t \frac{dl_3}{dt}\,dt'\right)$$

(14a)

$$A_{l_2l_3} = \left(\int_\tau^t \frac{dl_2}{dt}\,dt'\right)\left(\int_\tau^t \frac{dl_3}{dt}\,dt'\right)$$

(14b)

$$A_{l_1l_2} = \left(\int_\tau^t \frac{dl_1}{dt}\,dt'\right)\left(\int_\tau^t \frac{dl_2}{dt}\,dt'\right).$$

(14c)

Combining the Equations 11 and 14a–c, the total surface area, A_Y, of all product crystals is given by the following equation as a function of time:

$$A_Y = 2\int_0^t I_{Y,n}(\tau)[A_{l_1l_3} + A_{l_2l_3} + A_{l_1l_2}]\,d\tau.$$

(15)

In our model, we assume arbitrarily that the product crystals, Y, grow in all cases with their $A_{l_1l_2}$ surface in contact with the reactant. Therefore, the amount of sur-

face area of the reactant, X, that is covered by the growing product crystals, A_{cover}, is given by the following equation as a function of time:

$$A_{Y,\text{cover}} = \int_0^t I_{Y,n}(\tau)A_{l_1l_2}\,d\tau$$

$$= \int_0^t I_{Y,n}(\tau)\left(\int_\tau^t \frac{dl_1}{dt}\,dt'\right)\left(\int_\tau^t \frac{dl_2}{dt}\,dt'\right)d\tau$$ (16)

The total surface area of reactant X, A_X, that is still reactive at time, t, is, therefore, reduced and given by

$$A_X = A_X^0 - A_{Y,\text{cover}}$$

(17)

where A_X^0 is the initial surface area of the reactant, X. With these considerations, Equation 3 becomes

$$\frac{dc_i}{dt} = \frac{A_X}{M_f}k_X f_X(\Delta G) + \frac{A_{l_1l_2}}{M_f}k_{Yl_3}f_{Yl_3}(\Delta G')$$

$$+ 2\frac{A_{l_2l_3}}{M_f}k_{Yl_1}f_{Yl_1}(\Delta G') + 2\frac{A_{l_1l_3}}{M_f}k_{Yl_2}f_{Yl_2}(\Delta G')$$ (18)

Note that $A_{l_1l_2}$ is multiplied by 1 and not by 2 (one surface is attached to the surface of reactant X, thus not in contact with the fluid), and that ΔG is defined for dissolution and precipitation of X and $\Delta G'$ is defined for dissolution and precipitation of Y. If the kinetics are linear with respect to concentrations, then $f(\Delta G)$ can be obtained from:

$$f(\Delta G) = 1 - \frac{c_i}{c_{j,\text{eq}}} = 1 - \exp(\Delta G/RT)$$

(19)

Equation 18 was solved numerically using an implicit method for numerical stability. The input data are given in Table 2, and the three different heating histories that were used for the calculations are the same as those shown for the experiments in Figure 2. The heterogeneous nucleation behavior changes the kinetics significantly, as can be seen by a comparison of the results of the calculations (Figs. 5A–F and 7A–F).

For comparison, Figures 7A–F show the results of the calculations in the same way they were presented in Figures 5A–F (see above). The dramatic change in the results compared with the homogeneous nucleation is shown in particular in Figures 5E and 5F. The surface area of Y produced is higher in the case of a fast heating rate, but only at the beginning of the reaction. Different from the results of the homogeneous model, the surface area of Y produced in the case of the slow heating history reaches the amount of surface area already produced with the fast heating procedure after about 70 min. The difference of the results becomes even more obvious if the development of the Y volume is compared. After about 30 min a significant crossover occurs in terms of volume produced (Fig. 7F), which means that the calculations based on the slow heating procedure produce more product phase, Y, than those using the fast heating rate. Even if these results cannot be linked directly to the experimental results, the outcome of the model is in general agreement with the results of the experiments (Fig. 4). Of

course, the conditions and phases used in our computations produce a much faster reaction rate than could be observed in the experimental study of reaction R8. Time intervals of tens of minutes in the case of the calculation correspond to time intervals of tens of hours in the experiments. The results and their implications are discussed in detail below.

Fast heating procedure and temperature overshoot

Calculations were also done that used a third heating history, in which heating is also fast, and based on the experiments performed with a temperature overshoot of 10 °C (see above) during the first 50 min of the experiments (Fig. 2, dotted line). The calculations with this particular heating history were performed for both homogeneous as well as for heterogeneous nucleation behavior. The outcome of these calculations is shown in Figure 8.

DISCUSSION OF MODELING RESULTS

Both the homogeneous and heterogeneous nucleation models developed above provide reasonable explanations for the significant influence of heating rate on reaction rate. For all further considerations, we assume that the results of these models also can be used, at least in principle, to discuss the kinetic behavior of the more complicated mineral reaction studied experimentally. The variation in concentration (Figs. 5A and B and 7A and B) and ΔG (Figs. 5D and 7D) as a function of time show that the nucleation period starts earlier, but is shorter if the heating rate is increased (Figs. 5C and 7C). This early nucleation event, driven by a steep increase of ΔG, produces a larger number of nuclei and, therefore, a greater increase in the surface area of Y, compared with the case of slower heating rates (see Figs. 5E and 7E). Both models show that the nucleation rate, r_n, is higher using a faster heating rate.

Comparison of the results from homogeneous and heterogeneous nucleation models shows that there are important differences between the two. If the product crystals are growing independently of the surface of the reactant(s) (homogeneous nucleation), the faster heating rate causes a higher degree of conversion early in the experiment (Figs. 5E and F) because nucleation and growth of the product crystals start earlier than in the case of the slower heating procedure. However, as the experiment proceeds, this effect is reduced because the surface area of the reactants is also decreasing faster in the case of the faster heating, so that the fast and slow results yield similar rates. The length of time that is necessary to equalize the conversion depends on the reaction kinetics that are a function of the P-T-X conditions of the experiment and the heating rates used.

In the case of heterogeneous nucleation, the product crystals nucleate and grow on the surface of at least one of the reactants (Figs. 3A and B; Fig. 6), and the computed results are substantially different because varying nucleation rates (Figs. 5C and 7C) cause a different development of the reacting system. Figure 7F shows that
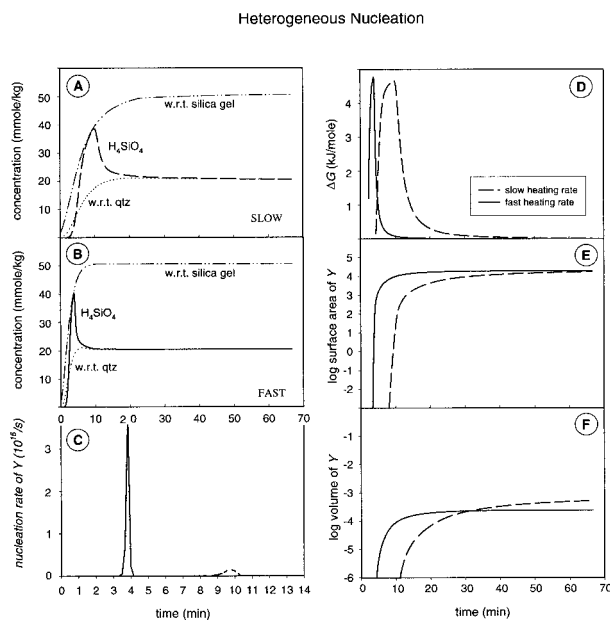

Heterogeneous Nucleation

FIGURE 7. Results of the simulation, assuming heterogeneous nucleation, i.e., the product Y (quartz) is growing on the surface of the reactant X (silica gel); results of slow heating procedure (dashed lines), and of fast heating procedure (solid lines). For more details see text. (**A**) Equilibrium concentrations of X (double dotted dashed line) and Y (dotted line) as a function of time, and the development of the concentration of H_4SiO_4 in the solution caused by the slow heating procedure; (**B**) Equilibrium concentrations of X and Y as a function of time, and the development of the concentration of H_4SiO_4 in the solution caused by the fast heating procedure; (**C**) Comparison of the nucleation rates of Y as a function of time for the slow and the fast heating rate; (**E**) Production of surface area of Y as a function of time; (**D**) ΔG-values as a function of time; (**F**) Production of volume of Y as a function of time. (The surface area of $\sqrt{y}$ is calculated in square centimeters, and the volume is calculated in cubic centimeters). The curves show a significant crossover after ~30 min.

in the first few minutes of reaction, the system displays behavior similar to the case of homogeneous nucleation (Fig. 5F), but after about 30 min the volume of Y produced by fast heating becomes less than that produced by slow heating. This is because higher nucleation rates cause surfaces of reactants to be covered faster, which results in a more rapid decrease of reactive surface area and decreased reaction rates. In addition, the morphology of the product crystals determines the rate of covering the surface: Plates will armor the surface faster than cubes and cubes faster than needles. The model used in this study considers anisotropic growth of product crystals and is, therefore, able to simulate different product morphologies (see Eq. 18). However, the armoring of the reactant surface decreases the total dissolution rate of the reactant. Therefore, the growth rate of the product crystals will decrease, too.

Figures 9A and B schematically show another important aspect of different nucleation rates, but assuming that
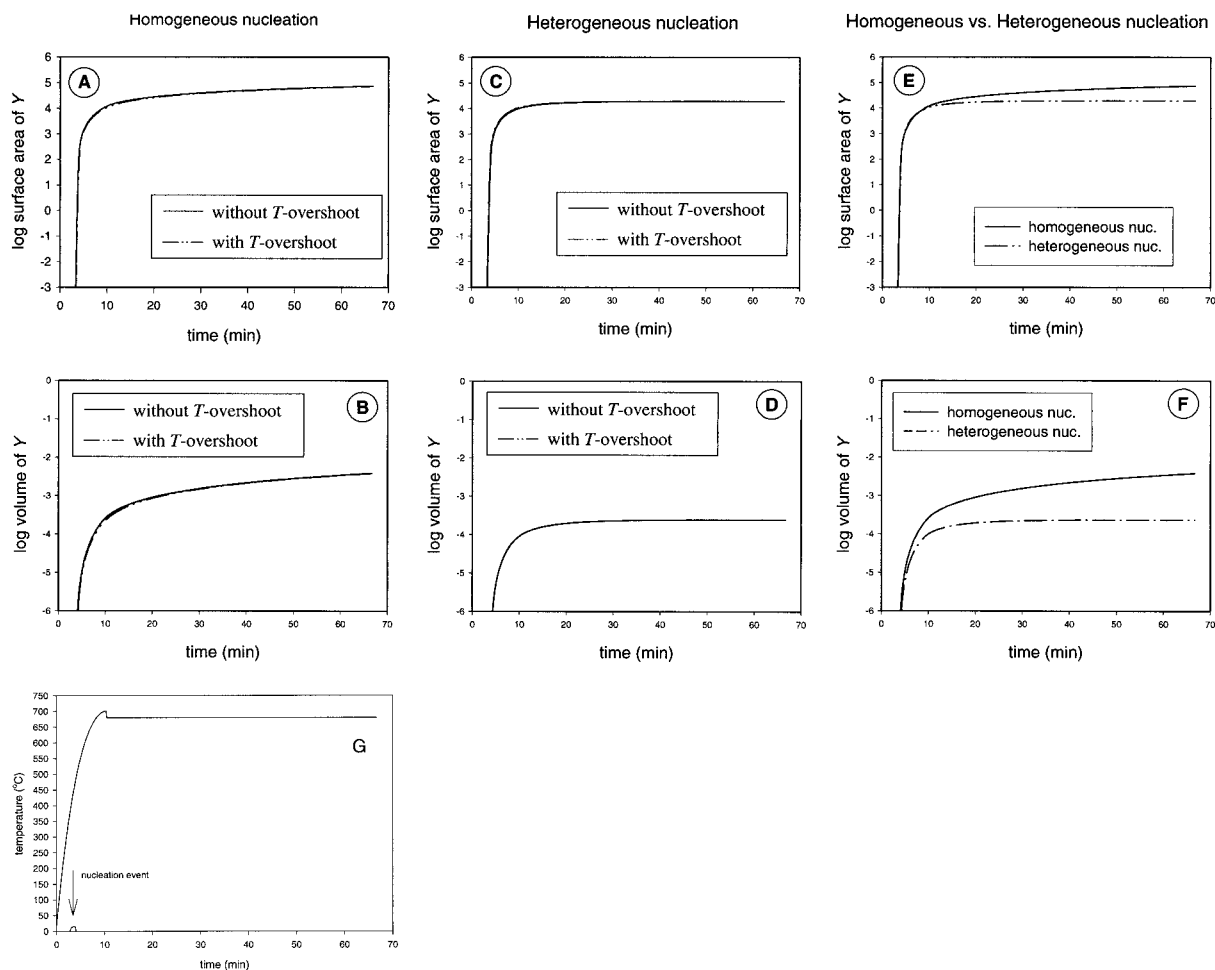
FIGURE 8. Results of the simulation, assuming that the product Y (quartz) is growing on the surface of the reactant X (silica gel), and assuming a heating procedure with a short temperature overshoot; (**A** and **B**) Development of the surface area and the volume of Y as $f(t)$ for the fast heating procedure with T overshoot (————·————), and without T overshoot (————), assuming homogeneous nucleation. (**C** and **D**) The same as in **A** and **B**, but assuming heterogeneous nucleation; (**E** and **F**) Comparison of results with a T overshoot for homogeneous and heterogeneous nucleation behavior; (**G**) Heating history and nucleation event for the heating procedure with a T overshoot. The nucleation is finished, before the temperature of the experiment is overshot.

the growth rates are the same: If many nuclei are formed (Fig. 9A) the layer of (meta)stable products will cover the surface of the reactant much faster (Fig. 9 at time, t_2) than in a case of a low nucleation rate (Fig. 9B). When the layer of product crystals completely covers the surface area of the reactants, the reaction becomes diffusion controlled, because the species have to diffuse through the armoring layer of product material. In Figures 9A and B, we compare the situation at t_1 (end of nucleation), t_2 (complete surface layer in the case of high nucleation rate), and t_3 (complete surface layer in the case of low nucleation rate) for both the slow and the fast heating rate. It is evident that in the case of a smaller number of nuclei (by slow heating) a larger volume of product can

be formed under surface control compared with the case with a higher nucleation rate (by fast heating).

As a consequence, we have to consider how two systems of identical chemical and mineralogical composition can develop differently. Such diverse outcomes can develop even if both systems reach identical P-T conditions, so long as the nucleation processes are slightly different. The difference in behavior becomes even stronger, if we consider carbonation, decarbonation, hydration, or dehydration reactions. In this case, the fluid composition will change, because different amounts of H_2O or CO_2 are produced or consumed by the reaction. Each change in fluid composition will change the actual temperature overstep, as long as the slope of the equilibrium curve is

not 0 (see Fig. 1) and the temperature of the experiment is constant. Therefore, the kinetics of the reaction can become significantly different in the two systems, even if the *P-T-X* conditions are constant and are controlled carefully during the experiment.

The SEM photomicrographs (Figs. 3A–D) of reaction mixtures of the decarbonation reaction studied here show that the product crystals (diopside and metastable talc + calcite) are growing nearly exclusively on dolomite surfaces. If the diopside crystals grow independently of the surfaces of the reactant, such as in some special diopside-seeded experiments of Lüttge and Metz (1991), the overall reaction rate is increased. The experimental results of that study are in good agreement with the simulation results. Therefore, the results of the simulation that incorporate heterogeneous nucleation are highly applicable to the experimental results discussed above: (1) A rapid heating rate decreases the reaction rate by increasing the nucleation rate of diopside crystals that grow on the dolomite surface, thereby reducing the reactive surface area and reaction rate. (2) A faster heating rate produces a shorter, more reproducible nucleation period than the conventional slower heating method. The uncertainty of the heating time is much larger in the latter case (± 10 min) compared with ± 0.5 min for the rapid heating rate. As a result, the scatter in conversion vs. time data decreases significantly.

Influence of temperature overshoot

Two different heating histories were compared in this simulation: (1) the fast procedure that was used before; and (2) a fast heating procedure with a short temperature overshoot (Fig. 8G). The simulations were done for both the homogeneous and the heterogeneous nucleation event.

Figures 8A–F show the outcome of these simulations: the log surface area and the log volume are plotted each as a function of time. Figures 8A and B show the results for the case of homogeneous nucleation, and Figures 8C and D show the case of heterogeneous nucleation. In Figures 8E and F, the two different nucleation events are compared directly, but only for the case of a temperature overshoot. All figures show clearly that the effect of the temperature overshoot is not significant if the overshoot happens when the nucleation event is finished (see Fig. 8G). The interesting fact is that the overshoot has a measurable influence on the kinetics only if the overshoot happens during the nucleation period. These results reflect again the effect that uncertainties in the heating procedure can cause. On the other hand, a very strict control of the experimental conditions at a later time cannot correct any mistakes produced in the beginning of an experiment. In general, these results also show the strong dependence on the difference of the Gibb's free energy, ΔG, of the reaction during the nucleation period.

It should be pointed out that there are also other experimental techniques that provide fast heating procedures, such as the piston cylinder apparatus (e.g., Johannes
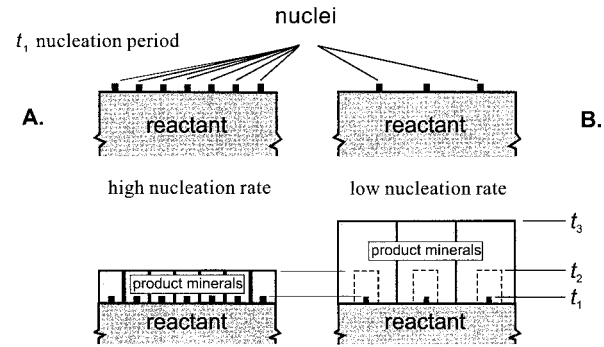

FIGURE 9. Sketch showing the different amount of product phase formed on a reactant surface as a result of two different nucleation rates. For simplicity only the top surface of the reactant is considered. (**A**) High nucleation rate; (**B**) Low nucleation rate; t_1 = end of nucleation period, t_2 and t_3 = two certain moments during the crystal growth process. (For detailed discussion see text).

1973), internally heated gas pressure vessels (e.g., Lofgren 1987), and cold seal pressure vessels in which the sample is levitated into position magnetically (e.g., Ihinger 1991). Each method has its own advantages, disadvantages, and limits: e.g., limited pressure-temperature range or costs. However, there are still many laboratories that use conventional externally heated hydrothermal apparatus in combination with cold-seal pressure vessels because of the ability to carry out many independent experiments simultaneously.

Application

Using rapid heating rates it is possible to investigate several problems in more detail. Examples include the initial stage of heterogeneous mineral reactions, even at a low overstepping of the equilibrium temperature (10–25 °C) (e.g., Lüttge and Neumann 1992; Lüttge et al. 1994) and the beginning of the product crystallization. The nucleation period can be determined more precisely as a function of the reaction temperature. Therefore, it is possible to get only the crystals (stable or metastable) that are first precipitated and to study them with SEM and other methods. A final example is the influence of surface properties on the reaction rate because a higher precision of conversion vs. time data is required to identify the influence of surface properties on the reaction kinetics.

We have shown experimentally and with computer simulations that the heating rate can have a significant influence on heterogeneous mineral reactions that are investigated on laboratory time scales (hours to months). The nucleation process in particular seems to be a key factor that is affected strongly by the rate of heating. An important question to ask is if these results may be applied to natural systems as well. Certainly, the application cannot be a direct one because heating rates in nature are orders of magnitude slower than in the laboratory. On the other hand, in the field we observe significant differences in textures of the same mineral assemblages at different

locations. Some contact metamorphic rocks show large single product crystals while others show an armoring rim of many small crystals around a reactant. Very commonly, both of these textures are developed in the same *P-T-X* range. This difference in the observed textures might be explained kinetically, specifically with differing nucleation rates. Therefore, we are developing computer models that simulate conditions closer to those found in nature (Lasaga and Lüttge, in preparation). Initial results do indicate an influence of heating rate on the kinetics of mineral reactions. However, much more work is necessary to achieve a better understanding of the processes that determine the structures of metamorphic rocks.

REFERENCES CITED

Bosbach, D. and Rammensee, W. (1994) In situ investigation of growth and dissolution on the (010) surface of gypsum by Scanning Force Microscopy. Geochimica et Cosmochimica Acta, 58, 843–849.

Burch, T.E., Nagy, K.L., and Lasaga, A.C. (1994) Free energy dependence of albite dissolution kinetics at 80C and pH 8.8. Chemical Geology, 105, 137–162.

Champness, P.E. and Brearley, A.J. (1986) Experimental studies of reaction mechanisms and problems of extrapolating kinetic data in the pressure-temperature plane. International Symposium of Experimental Mineralogy and Geochemistry, Nancy, France, 118–119.

Dachs, E. and Metz, P. (1988) The mechanism of the reaction 1 tremolite + 3 calcite + 2 quartz = 5 diopside + 3 CO_2 + 1 H_2O: results of powder experiments. Contributions to Mineralogy and Petrology, 100, 542–551.

Dove, P.M. and Hochella, M.F., Jr. (1993) Calcite precipitation mechanisms and inhibition by orthophosphate: In situ observations by Scanning Force Microscopy. Geochimica et Cosmochimica Acta, 57, 705–714.

Dove, P.M. and Rimstidt, J.D. (1994) Silica-water interactions. In Mineralogical Society of America Reviews in Mineralogy, 29, 259–308.

Gottschalk, M. (1990) Internally consistent thermodynamic data in the system SiO_2-Al_2O_3-CaO-MgO-K_2O-Na_2O-H_2O-CO_2. Ph.D. thesis, Eberhard-Karls Universität, Tübingen, Germany (in German).

——— (1997) Internally consistent thermodynamic data for rock forming minerals. European Journal of Mineralogy, 9, 175–223.

Gratz, A.J., Manne, S., and Hansma, P.K. (1991) Atomic Force Microscopy of atomic-scale ledges and etch pits formed during dissolution of quartz. Science, 251, 1343–1346.

Heinrich, W., Metz, P., and Bayh, W. (1986) Experimental investigation of the mechanism of the reaction: 1 tremolite + 11 dolomite = 8 forsterite + 13 calcite + 9 CO_2 + 1 H_2O. Contributions to Mineralogy and Petrology, 93, 215–221.

Heinrich, W., Metz, P., and Gottschalk, M. (1989) Experimental investigation of the kinetics of the reaction: 1 tremolite + 11 dolomite = 8 forsterite + 13 calcite + 9 CO_2 + 1 H_2O. Contributions to Mineralogy and Petrology, 102, 163–173.

Ihinger, P.D. (1991) An experimental study of the interaction of water with granitic melt, 190 p. Ph.D. thesis, California Institute of Technology, Pasadena, California.

Johannes, W. (1973) A simplified piston-cylinder apparatus of high precision. Neues Jahrbuch, Monatshefte, 373–351 (in German).

Käse, H.-R. and Metz, P. (1980) Experimental investigation of the metamorphism of siliceous dolomites. Contributions to Mineralogy and Petrology 73, 151–159.

Kerrick, D.M., Lasaga, A.C., and Raeburn, S.P. (1991) Kinetics of heterogeneous reactions. In Mineralogical Society of America Reviews in Mineralogy, 26, 583–671.

Lasaga, A.C. (1981) Rate laws of chemical reactions. In Mineralogical Society of America Reviews in Mineralogy 8, 1–68.

——— (1984) Chemical kinetics of water-rock interactions. Journal of Geophysical Research, 89, B6, 4009–4025.

——— (1998) Kinetic theory and applications in earth sciences, 600 p. Princeton Press, Princeton.

Lasaga, A.C. and Rye, D.M. (1993) Fluid flow and chemical reactions in metamorphic systems. American Journal of Science, 293, 361–404.

Lasaga, A.C., Soler, J.M., Ganor, J., Burch, T.E., and Nagy, K.L. (1994) Chemical weathering rate laws and global geochemical cycles. Geochimica et Cosmochimica Acta, 58, 2361–2386.

Lofgren, G. (1987) Internally heated systems. In G.C. Ulmer, and H.L. Barnes, Eds., Hydrothermal Experimental Techniques, p. 324–332. Wiley, New York.

Lüttge, A. and Metz, P. (1991) Mechanism and kinetics of the reaction: 1 dolomite + 2 quartz = 1 diopside + 2 CO_2 investigated by powder experiments. In T.M. Gordon and R.F. Martin, Eds., Quantitative Methods in Petrology; an issue in honor of Hugh J. Greenwood. Canadian Mineralogist, 29, 803–821.

——— (1993) Mechanism and kinetics of the reaction: 1 dolomite + 2 quartz = 1 diopside + 2 CO_2: a comparison of rock-sample and of powder experiments. Contributions to Mineralogy and Petrology, 115, 155–164.

Lüttge, A. and Neumann, U. (1992) The initial stage of a heterogeneous mineral reaction: Experimental investigations of the determining parameters. Geological Society of America Abstracts with Programs, 24, 255–256.

——— (1993). Side reactions: An experimental study of metastable phase formation. Geological Society of America Abstracts with Program, 25, 214.

Lüttge, A., Neumann, U., and Jenkins, D.M. (1994) Is the initial stage of heterogeneous mineral reactions the key understanding the kinetics? Geological Society of America Abstracts with Program, 26, 290.

Lüttge, A., MacInnis, I.N., and Lasaga, A.C. (1996) A new experimental technique to quantify surface dynamics of silicates at near atomic scale using in situ optical interferometry. Berichte der Deutschen Mineralogischen Gesellschaft, Beiheft zum European Journal of Mineralogy 8/1, 176.

MacInnis, I.N. and Brantley, S.L. (1992) The role of dislocations and surface morphology in calcite dissolution. Geochimica et Cosmochimica Acta 56, 1113–1126.

MacInnis, I.N., Lüttge, A., and Lasaga, A.C. (1996) New surface experimental technique using interferometry for in situ measurement of silicates dissolution/precipitation kinetics at hydrothermal conditions. Geological Society of America Abstracts, 28, 146.

Matthews, A. (1980) Influence of kinetics and mechanism in metamorphism: a study of albite crystallization. Geochimica et Cosmochimica Acta 44, 387–402.

——— (1985) Kinetics and mechanisms of the reaction of zoisite to anorthite under hydrothermal conditions: reaction phenomenology away from the equilibrium region. Contributions to Mineralogy and Petrology, 89, 110–121.

Matthews, A. and Goldsmith, J.R. (1984) The influence of metastability on reaction kinetics involving zoisite formation from anorthite at elevated pressures and temperatures. American Mineralogist, 69, 848–857.

Nagy, K.L. and Lasaga, A.C. (1992) Dissolution and precipitation kinetics of gibbsite at 80 C and pH 3: The dependence on solution saturation state. Geochimica et Cosmochimica Acta, 56, 3093–3111.

Neumann, U. and Lüttge, A. (1995) The importance of the conditioning of reactant surfaces in powder experiments. Berichte der Deutschen

Mineralogischen Gesellschaft, Beiheft zum European Journal of Mineralogy, 7/1, 177.

Putnis, A., Junta-Rosso, J.L., and Hochella, M.F., Jr. (1995) Dissolution of barite by a chelating ligand: An atomic force microscopy study. Geochimica et Cosmochimica Acta, 59, 4623–4632.

Rimstidt, J.D. and Barnes, H.L. (1980) The kinetics of the silica-water reactions. Geochimica et Cosmochimica Acta, 44, 1683–1699.

Rubie, D.C. and Thompson A.B. (1985) Kinetics of metamorphic reactions at elevated temperatures and pressures: an appraisal of available experimental data. In A.B. Thompson and D.C. Rubie, Eds., Metamorphic Reactions: Kinetics, Textures and Deformation, Advances in Physical Geochemistry, 4, 27–79. Springer, New York.

Schramke, J.A., Kerrick, D.M., and Lasaga, A.C. (1987) The reaction muscovite + quartz = andalusite + K-feldspar + water. Part 1. Growth kinetics and mechanism. American Journal of Science, 287, 517–559.

Stipp, S.L.S., Eggleston, C.M., and Nielsen, B.S. (1994) Calcite surface structure observed at microtopographic and molecular scales with atomic force microscopy (AFM). Geochimica et Cosmochimica Acta, 58, 3023–3033.

Tanner, S.B., Kerrick, D.M., and Lasaga, A.C. (1985) Experimental kinetic study of the reaction: calcite + quartz = wollastonite + carbon dioxide, from 1 to 3 kilobars and 500° to 850 °C. American Journal of Science, 285, 577–620.

Weast, R.C. (Ed.) (1992) CRC Handbook of Chemistry and Physics, (73rd edition), CRC Press, Boca Raton.

Widmer, J., Metz, P., and Lüttge, A. (1995) Kinetics of the formation of talc in siliceous dolomites. Terra abstracts, 7, 152–153.

Winkler, U. and Lüttge, A. (1997) Experiments on the kinetics of the metamorphic reaction 1 tremolite + 3 calcite + 2 quartz = 5 diopside + 3 CO_2 + 1 H_2O with special focus on the influence of a chloridic fluid phase. Terra abstracts, 9, 570.